Journal Pre-proof

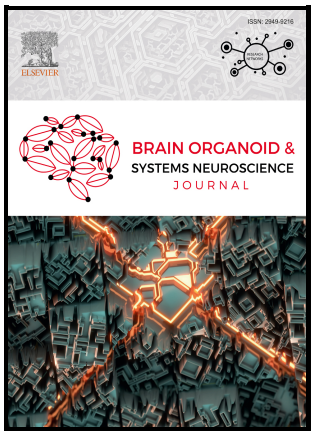

Impact of Unilateral Maximal Dentate Activation on Nitrergic Neuron Distribution in the Hippocampus, Entorhinal cortex, Amygdala and Habenula

Cristiano Bombardi, Roberto Colangeli, Maurizio Casarrubea, Philippe De Deurwaerdère, Vincenzo Crunelli, Giuseppe Di Giovanni

PII: S2949-9216(25)00026-2

DOI: https://doi.org/10.1016/j.bosn.2025.100038

Reference: BOSN100038

To appear in: *Brain Organoid and Systems Neuroscience Journal*

Received date: 16 October 2025
Revised date: 6 December 2025
Accepted date: 14 December 2025

Please cite this article as: Cristiano Bombardi, Roberto Colangeli, Maurizio Casarrubea, Philippe De Deurwaerdère, Vincenzo Crunelli and Giuseppe Di Giovanni, Impact of Unilateral Maximal Dentate Activation on Nitrergic Neuron Distribution in the Hippocampus, Entorhinal cortex, Amygdala and Habenula, *Brain Organoid and Systems Neuroscience Journal,* (2025) doi:https://doi.org/10.1016/j.bosn.2025.100038

Systems and Organoids.

Impact of Unilateral Maximal Dentate Activation on Nitrergic Neuron Distribution in the Hippocampus, Entorhinal cortex, Amygdala and Habenula

Cristiano Bombardi[1], Roberto Colangeli[2,3], Maurizio Casarrubea[4], Philippe De Deurwaerdère[5], Vincenzo Crunelli[6,7], Giuseppe Di Giovanni[2,6,8,9*]

[1]Department of Veterinary Medical Science, University of Bologna, Bologna, Italy; [2]Laboratory of Neurophysiology, Department of Physiology and Biochemistry, Faculty of Medicine and Surgery, University of Malta, Msida, Malta. [3] UniCamillus, International Medical University in Rome, Rome, Italy. [4]Laboratory of Behavioral Physiology, Department of Biomedicine, Neuroscience and Advanced Diagnostics (Bi.N.D.), Human Physiology Section "Giuseppe Pagano", University of Palermo, Palermo, Italy. [5]University of Bordeaux, France; Centre National de la Recherche Scientifique (CNRS), Unit 5287, Institut des Neurosciences Intégratives et Cognitives d'Aquitaine (INCIA), Bordeaux, France. [6]Neuroscience Division, School of Biosciences, Cardiff University, Cardiff, United Kingdom. [7]Department of Pharmacology and Neuroscience, Faculty of Medicine, Lisbon University, Lisbon, Portugal. [8]College of Medicine, Korea University, Seoul 02841, Republic of Korea. [9]Department of Medical and Surgical Sciences, University of Magna Graecia, Catanzaro, Italy

*Corresponding author: Giuseppe Di Giovanni, giuseppe.digiovanni@unicz.it

Funding

This work was supported by grant PHBRP08-05 from the University of Malta, Malta and by internal funds from the University of Bologna, Italy.

CRediT authorship contribution statement

Cristiano Bombardi: Investigation, Methodology, Visualization, Writing – review & editing. **Roberto Colangeli**: Investigation, Methodology, Visualization, Formal analysis, Software, Data curation. **Maurizio Casarrubea**: Writing –review & editing. **Philippe De Deurwaerdère**: Writing – review & editing. **Vincenzo Crunelli**: Writing – review & editing. **Giuseppe Di Giovanni**: Conceptualization, Supervision, Writing – review & editing.

Declaration of Competing Interest

The authors declare no conflict of interest.

ABSTRACT

Mesial temporal lobe epilepsy (mTLE) is the most common form of epilepsy involving the hippocampus. While hippocampal circuits have been extensively studied, increasing evidence suggests that extrahippocampal structures, including the amygdala and habenula, may contribute to seizure propagation and epileptogenesis. Among modulators of excitability, nitric oxide (NO) is a key regulator, although its role in mTLE remains controversial, with both pro- and anticonvulsant effects reported.

We used maximal dentate activation (MDA) in the dentate gyrus, elicited by repeated unilateral perforant path stimulation in rats, a well-established model for studying early mechanisms of epileptogenesis in mTLE. Repeated stimulation progressively shortened MDA onset latency and prolonged seizure duration, reflecting enhanced network excitability. To assess acute nitrergic alterations, an exploratory neuronal NO synthase (nNOS) and NADPH-diaphorase (NADPH-d) histochemical study wase performed in the hippocampus, entorhinal cortex, amygdala and habenula to determine whether repeated seizures could induce early changes in nitrergic neuronal expression.

Histochemical analysis revealed region- and layer-specific changes in nitrergic neurons after MDA. In CA1 and CA3, reductions were observed in the stratum oriens, accompanied by an increased density in the CA3 pyramidal layer. The subiculum exhibited a depletion driven by a decrease of nitrergic neurons in the hemisphere contralateral to the stimulation, whereas the entorhinal cortex, basolateral amygdala and medial habenula were largely unaffected. In the lateral habenula, MDA did not alter the overall mean of the density of nitrergic neurons, but it increased it in the stimulated hemisphere and decreased it in the contralateral one.

This preliminary study reveals adaptations that may indicate a sensitivity of nitrergic neurons to paroxysmal dentate activity and provide a basis for further exploring the potential involvement of NO-related pathways in limbic network responses and TLE-relevant mechanisms and treatments.

Key Words: Neuronal nitric oxide synthase (nNOS); Lateral habenula; Dentate gyrus; Nitric oxide (NO); Mesial temporal lobe epilepsy (mTLE); Epileptogenesis;

Introduction

Epilepsy is one of the most prevalent chronic neurological disorders, affecting approximately 1% of the global population (Feigin, Vos et al. 2025). Mesial temporal lobe epilepsy (mTLE) is the most common form of focal epilepsy in adults, often associated with hippocampal sclerosis and progressive network reorganization (Téllez-Zenteno and Hernández-Ronquillo 2012). It is characterized by spontaneous recurrent seizures resulting from abnormal, synchronized, high-frequency neuronal discharges (Carter, Deshpande et al. 2011). The epileptogenic process is typically initiated by an acute brain insult, such as trauma, status epilepticus, or infection, followed by a clinically silent period during which molecular, cellular, and structural changes promote chronic hyperexcitability (Park 2024). Neuroinflammatory mechanisms, gliosis, and maladaptive synaptic plasticity contribute both to seizure generation and to comorbid cognitive and affective disturbances (Ravizza, Scheper et al. 2024, Hollis and Lukens 2025).

Among neuromodulatory systems implicated in epilepsy, nitric oxide (NO) has received considerable attention. NO is a gaseous messenger produced by nitric oxide synthase (NOS) isoforms, with neuronal NOS (nNOS) being the calcium/calmodulin-dependent form constitutively expressed in select neuronal populations (Bredt, Glatt et al. 1991, Pierucci, Galati et al. 2011, Chachlaki and Prevot 2020). The hypothesis that NO functions as an endogenous antiepileptic agent has yielded conflicting results. Some recent studies report that NO donors are antiepileptogenic (Zhu, Zhou et al. 2025) while hilar nitrergic interneurons degeneration represents a pathological hallmark of mTLE in patients (Zhu, Zhou et al. 2025) and animal models (Wang, Zhang et al. 2021, Zhu, Zhou et al. 2025). Consistently, NOS inhibition can worsen seizures or facilitate epileptiform burst initiation (Del-Bel, Oliveira et al. 1997, Alabadí, Thibault et al. 1999). Conversely, other work suggests NOS inhibition suppresses seizures (Sardo, Carletti et al. 2006).

While the hippocampus remains the primary focus in mTLE, extrahippocampal structures also contribute to seizure networks, such as the amygdala (Aung, Tang et al. 2025, Takeyama, Matsumoto et al. 2025, Venkatesan, Babajani-Feremi et al. 2025) and the medial and lateral habenula (Patel, Millan et al. 1988, De Sarro, Meldrum et al. 1992, Takechi, Suemaru et al. 2016). However, changes in nitrergic neurons in mTLE network remain largely unexplored, with early work by Stringer and Erden (Stringer and Erden 1990) focused on hippocampus showing selective loss in the dentate gyrus and hemisphere-specific vulnerability after repeated seizures.

To address this gap, we used unilateral electrical maximal dentate activation (MDA) in anesthetized rats, an acute kindling paradigm reproduced key features of mTLE (Stringer and Lothman 1989, Stringer and Lothman 1992, Orban, Pierucci et al. 2013, Orban, Bombardi et al. 2014, Colangeli, Pierucci et al. 2017). We then examined nNOS-positive neurons in the hippocampus and

extrahippocampal limbic structures involved in seizure networks, i.e., the amygdala, the medial and lateral habenula (MHb and LHb). Our histochemical studies revealed region-specific alterations in nitrergic neurons, particularly within the hippocampus but not in the amygdala and MHb. Notably, asymmetric alterations were observed in the LHb, suggesting its involvement in MDA seizure propagation. Taken together, these findings provide novel insights into the distribution of the NO system under both physiological conditions and seizure-induced network changes. Although preliminary, they offer a foundation for further exploring the potential involvement of NO-related pathways in limbic network dynamics and mTLE-relevant mechanisms.

Experimental procedures

Animals

Male Sprague-Dawley rats (Charles River, Italy), weighing 250-300 g, were used in this study. All procedures involving animals complied with Council Directive 86/609/EEC, the Animals (Scientific Procedures) Act 1986, and local regulations on the use of animals in research. Rats were anesthetized with urethane (1.2 g/kg, i.p.; Sigma-Aldrich Co., Milano, Italy) and positioned in a stereotaxic frame. Body temperature was maintained at 37 °C using a heating pad and a temperature controller unit (Temperature Control Unit HB 101/2, Letica Scientific Instruments). Surgical procedures and recordings of field potentials were carried out as previously described (Orban, Pierucci et al. 2013, Orban, Bombardi et al. 2014). In brief, the population spike (PS) was elicited by stimulating the right medial perforant path (PP; coordinates AP: −8.3, L: 4.8, V: 3.4) using a bipolar stimulating electrode (bifilar stainless-steel wire, CFW, CA, USA). The recording electrode was placed in the right hilus of the dentate gyrus (DG) of the hippocampus (AP: −4.8, L: 2.2, V: 3.6). Electrical signals were amplified with a NeuroLog amplifier (Digitimer Ltd; high-pass: 0.2 Hz, low-pass: 5000 Hz, gain: 200). Square-wave pulses of 0.3 ms duration were delivered at a rate of 1/min using a digitally controlled constant current stimulator (Digitimer Ltd, DS3).

The PS amplitude was measured and stimulus intensity was adjusted to evoke 45-50% of the maximal PS response. Signals were digitized with a CED 1401 Plus A/D converter (Cambridge Electronic

Design Ltd., UK), stored on a computer, and analyzed offline using Signal 1.9 software at a sampling rate of 10 kHz. Electrode placement was confirmed by histological examination (not shown).

Maximal Dentate Activation

Induction of MDA began once normal excitability of the DG was confirmed, typically 30 min or more after surgery. Excitability was assessed using paired-pulse stimulation with two different interpulse intervals (25 ms and 150 ms), which preferentially evoke fast inhibition and facilitation, respectively (Orban, Pierucci et al. 2013, Di Giovanni, García et al. 2014). MDA was identified electrophysiologically based on established criteria (Stringer and Lothman 1989, Orban, Pierucci et al. 2013, Di Giovanni, García et al. 2014, Orban, Bombardi et al. 2014, Colangeli, Pierucci et al. 2017, Grillo, Fezza et al. 2021). Seizure-inducing stimulus trains were repeated every 10 min for 4 h, totaling 24 trains. Latency to MDA onset was defined as the time from stimulus onset to the appearance of a PS with half-maximal amplitude (Figure 1B), corresponding to a rise of extracellular potassium and a negative shift of the dc potential (Stringer and Lothman 1992, Orban, Pierucci et al. 2013, Orban, Bombardi et al. 2014, Colangeli, Pierucci et al. 2017).

After six stimulus trains, MDA duration progressively increased while onset latency decreased over repeated stimulations (Stringer and Lothman 1990, Orban, Pierucci et al. 2013). To allow comparisons across animals, MDA durations and onset latencies were "normalized" by subtracting values measured in response to the first stimulus train from those measured in subsequent trains. This approach enabled calculation of changes in MDA duration or onset time for each train relative to the initial response, allowing group averages and comparisons to be made (see (Stringer and Lothman 1990, Orban, Pierucci et al. 2013, Orban, Bombardi et al. 2014).

Animal perfusion and brain fixation

Six Sprague–Dawley rats, three sham control (CTL) and three undergone MDA protocol for 4h (MDA) were used in this study. The animals were deeply anesthetized with a mixture (4.0 ml/kg) of sodium pentobarbital (48 mg/kg) and chloral hydrate (40 mg/kg; intraperitoneally) and perfused through the ascending aorta by using a peristaltic pump (flow rate 30-35 ml/min) as follows: 0.9% saline (+ 4°C) for 2 minutes, followed by a solution of 4% paraformaldehyde in 0.1 M sodium phosphate buffer, pH 7.4 (flow rate 10 ml/min) for 30 min. The brains were removed from the skull and postfixed in the final fixative for 2 to 4 h. The brains were then cryoprotected in 30% sucrose solution in phosphate buffered saline (PBS), pH 7.4 at + 4° C for 48 h and cut in the coronal plane at 30 μm section thickness on a freezing sliding microtome. The sections (1 in 5 series) were stored in

30% sucrose solution in PBS at –20°C (for immunohistochemical staining) or in 10% formalin at room temperature (for thionin staining) until processed.

Immunoperoxidase

The free-floating coronal sections were washed three times (10 min each time) in 0.02 M PBS, pH 7.4. To eliminate endogenous peroxidase activity, the sections were treated with 1% H_2O_2 in H_2O for 15-30 min, and then rinsed 6 times in 0.02 MPBS. To reduce non-specific binding, the sections were incubated in a solution containing 10% normal goat serum (Colorado Serum Co., Denver, CO, #CS 0922) and 0.3% Triton X-100 in 0.02 M PBS for 2 h at room temperature. Thereafter, the sections were incubated in a solution mouse monoclonal antibody anti-nNOS (diluted 1:100; Santa Cruz Biotechnology sc-5302; Santa Cruz, CA, USA), 0.3% Triton X-100, and 1% normal goat serum for 48 h at 4°C (the final concentrations of primary antibodies were established by performing immunoperoxidase using different dilution pattern). Following incubation in the primary antiserum, the sections were washed three times for 10 minutes each in 0.02 M PBS containing 2% normal goat serum. The sections were incubated in a solution containing goat biotinylated anti-mouse (1:200, Vector, Burlingame, CA, BA-9200), 1% normal goat serum, and 0.3% Triton X-100 in 0.02 M PBS, pH 7.4 for 60 min at room temperature. The sections were again washed three times for 10 min each in 0.02 M PBS containing 2% normal goat serum and transferred to avidin-biotin complex (ABC kit Vectastain, PK-6100,Vector, Laboratories, Burlingame, CA) for 45 min. The sections were washed three times in 0.02 M PBS, pH 7.4 and immunoperoxidase reaction was developed by 3.30-diaminobenzidine (DAB kit, SK-4100, Vector, Laboratories,Burlingame, CA). After washing, the sections were mounted onto gelatin-coated slides, dried overnight at 37°C, defatted, and cover slipped with DePeX (BDH Laboratory Suplies Poole, England).

Specificity of the mouse anti-nNOS was obtained by detecting a NADPH-d histochemical reaction in sections initially stained against nNOS. In particular, sections were incubated in 0.1 M Tris buffer (pH 8.0) containing 1 mM b-NADPH (Sigma N-1630), 0.1 mM nitroblue tetrazolium (Sigma N-6876), and 0.3% Triton X-100 for 1 h at 37° C. After washing in 0.3% Triton X-100 in Tris-buffered saline, the sections were dried overnight, dehydrated in ethanol, cleared in xylene, and cover slipped with Entellan (Merck, Darmstaldt, Germany). The NADPH-d reaction and the mouse anti-nNOS marked the same somata. Incubation without the substrate NADPH or without the electron acceptor NBT reduced NADPH-d staining. This aspect demonstrated the specificity of NADPH-d histochemical staining. In addition, control sections incubated without the primary antibody resulted in a complete disappearance of stained profiles. The omission as well as the replaced of the secondary

antibodies with inappropriate secondary antibodies resulted in elimination of all immunoistochemical staining.

Other stainings

To help identify the cytoarchitectonic boundaries of different amygdaloid nuclei, one series of sections was stained with thionin as follows. Sections were taken out of the 10% formaldehyde solution, mounted on gelatin-coated slides, and dried overnight at 37 ◦C. Sections were defatted 1 h in a mixture of chloroform/ethanol 100% (1:1), and then rehydrated through a graded series of ethanol, 2×2 min in 100% ethanol, 2 min in 96% ethanol, 2 min in 70% ethanol, 2 min in 50% ethanol, 2 min in dH2O, and stained 30 s in a 0.125% thionin (Fisher Scientific)solution, dehydrated and coverslipped with DPX (BDH Laboratory Suplies Poole, England).

Histochemical analysis

Sections were analyzed using a Leica DMRB microscope. Brightfield images were acquired by means of a Polaroid DMC digital camera (Polaroid Corporation, Cambridge, MA, USA) and DMC 2 software. Contrast and brightness were adjusted to reflect the appearance of the labeling seen through the microscope using Adobe Photoshop CS3 Extended 10.0 software (Adobe Systems, San Jose, CA).

To calculate the density nNOS-immunoreactive (nNOS-IR) neurons in dentate gyrus, hippocampus proper (CA3, CA1), subiculum, entorhinal cortex and habenular complexes, immunostained neurons were plotted in every fifth section throughout each area with a computer-aided digitizing system (Accustage 5.1, St. Shoreview, MN). The boundaries of the dentate gyrus, hippocampus proper, subiculum, entorhinal cortex, basolateral nuclear complex of the amygdala and habenular complexes were drawn from the adjacent thionin-stained sections using a stereo microscope equipped with drawing tube and confirmed using standard atlas references (Paxinos and Watson 2004). The outlines were superimposed on computer generating plots using Corel Draw X3 (Corel corporation, Ottawa, Ontario, Canada). The density of nNOS-IR neurons in the different areas was calculated as number of neurons/mm^2 in each section separately. A mean density of positive neurons was obtained by counting the mean number of positive cells in 5 successive sections (1 in 5 series). The area measurements were done from the line drawings by using AxioVision Rel.4.8 (Zeiss). The groups were: sham control (CTL, average from both left and right hemisphere), CTL-L (left hemisphere) and CTL-R (right hemisphere, ipsilateral to the electrodes); MDA (average from both left and right hemisphere) and MDA-L and MDA-R (average from left and right hemisphere, respectively).

Neuropil staining intensity was assessed using a three-level semi-quantitative scale: (+) low (sparse, faint labeling), (++) moderate (continuous labeling of intermediate intensity), and (+++) high (dense, strong diffuse staining). Scoring was performed by two blinded observers.

Statistics

Statistical analyses and figures were performed using GraphPad Prism 9.5 (San Diego, CA). For each brain area, nitrergic neuron density was quantified in five systematically sampled sections per hemisphere, and the mean hemispheric value per animal was used for statistical analysis. The animal was considered the independent biological replicate, whereas left and right hemispheric values were treated as within-animal dependent measures but independent across animals. CTL vs MDA comparisons were analyzed using an unpaired two-tailed t-test with Welch's correction. Comparisons between left and right hemispheres within the same experimental group were performed using paired two-tailed t-tests and p values were adjusted using the Holm–Šidák correction for multiple testing. Cohen's d was calculated as a measure of effect size (calculated in Microsoft Excel). Data are expressed as mean ± SD, and statistical significance was defined as $p < 0.05$.

Results

Maximal dentate activation

The change in MDA duration progressively increased over the first 12 stimulus trains, then became more variable, reaching 24.5 ± 2.4 s by the 24th train. Onset latency showed a gradual decline, reaching 2.2 ± 0.3 s at the eighth train before plateauing (Fig. 1A, B) (n = 6).

Distribution of nNOS immunoreactivity in the dentate gyrus, hippocampus proper, subiculum and entorhinal cortex

Dentate Gyrus

In control sham rats, numerous nitrergic neurons were observed in the polymorphic and granule cell layers (Fig. 2A1, B1; Table 1). Cells in the polymorphic layer were large and multipolar, while those in the granule cell layer, particularly near the hilar border (subgranular zone), displayed fusiform or pyramidal morphology with prominent apical dendrites extending into the molecular layer. Neurons of the subgranular zone had large fusiform somata with dendrites running parallel to the granule cell layer. Rare multipolar cells were found in the molecular layer.

The neuropil contained many nNOS-IR dendritic profiles in the polymorphic cell layer, with strong diffuse staining in the molecular layer, especially near the granule cell layer. Semi-quantitative evaluation confirmed moderate-to-strong neuropilar density in both the polymorphic and molecular layers, whereas the granule cell layer showed low labeling (Table 2).

Following MDA induction, a reduction in nitrergic neurons was observed in the polymorphic cell layer, granular cell layer and molecular layer compared with controls; however, this effect did not reach statistical significance, likely reflecting limited statistical power. Similarly, the granule cell layer showed no overall difference between the density of nitrergic neurons of CTL and MDA animals, and although a degree (non-significant) of lateralization was present, with nitrergic neurons more abundant contralateral (MDA L) than ipsilateral (MDA R) to the PP stimulation (Table 1). The molecular layer was not affected by the induction of MDAs. Consistent with this lack of effect, neuropilar density in the DG remained largely preserved across groups (Table 2).

Hippocampus Proper

In controls, nitrergic neurons were mainly localized to the pyramidal cell and radiatum layers, with a moderate number in the stratum oriens and virtually none in the stratum lacunosum-moleculare (Fig. 2A1, C1) (Table 1). Cells in the pyramidal layer were predominantly bipolar, extending dendrites

into strata oriens and radiatum, although occasional multipolar cells were also noted. Radiatum neurons were typically large and multipolar or fusiform, sometimes positioned near the border with lacunosum-moleculare. Neurons in oriens had both multipolar and bipolar morphologies.

Strong neuropilar staining was present in strata oriens and radiatum, especially near the lacunosum-moleculare, which also contained many immunoreactive axons. According to the semi-quantitative analysis (Table 2), neuropil density was moderate-to-high in stratum oriens and radiatum, low in the pyramidal layer, and weak-to-moderate in the lacunosum-moleculare.

After MDA, CA1 stratum oriens showed a significant reduction in nitrergic neurons compared to controls ($t_{(3.63)} = 3.53$, $p < 0.05$, $d = 2.89$). In this region, a trend toward reduced values was observed in the right hemisphere of MDA rats compared with the left, although this did not reach statistical significance after correction ($t_{(2)} = 3.38$, $p = 0.1487$, $d = 1.95$). A marked reduction was present in the right hemisphere of MDA rats compared with CTL ($t_{(3.96)} = 5.88$, $p < 0.05$, $d = 4.80$), whereas the difference between CTL-L and MDA-L did not survive multiple-comparison correction ($t_{(2.31)} = 3.48$, $p = 0.1487$, $d = 1.89$) (table 1). The CA1 pyramidal layer remained largely preserved. In CA3, the stratum oriens showed a marked loss of nitrergic neurons ($t(3.95) = 15.84$, $p < 0.05$, $d = 12.93$), and this effect regarded both MDA hemisphere. On the other hand, the pyramidal layer displayed an increased density compared to controls ($t_{(4.00)} = -4.13$, $p < 0.05$, $d = 3.37$). In both CA1 and CA3, the neuropilar distribution remained comparable to controls (Table 2), suggesting that the nitrergic neuron processes are more resilient than cell bodies to MDA-induced alterations.

Subiculum

In control animals, nitrergic neurons were distributed throughout all subicular layers, displaying bipolar, multipolar, and pyramidal morphologies, with dense neuropil staining particularly evident in layer III. Overall, the neuropil exhibited high to very high density, forming an intricate network consistent with the subiculum's role as a major hippocampal output structure (Table 2).

A reduction in nitrergic neuron density was observed in the subiculum of MDA rats compared to control animals ($t_{(3.71)} = 3.66$, $p < 0.05$, $d = 2.99$; Fig. 3B1; Table 1). No significant difference was detected between the left and right subiculum within the MDA group, nor no significant difference was observed in the right subiculum between CTL and MDA animals. In contrast, a significant reduction in nitrergic neurons was found in the left subiculum of MDA rats compared to CTL ($t_{(2.20)} = 7.96$, $p < 0.05$, $d = 6.50$). Overall, these results indicate that the decrease in nitrergic neurons in the subiculum is mainly attributable to a contralateral reduction relative to the side of stimulation following repeated MDA discharges (Table 1). Despite this left-hemisphere reduction, neuropil

staining in MDA rats remained moderate to strong in most layers (Table 2), indicating a partial preservation of nitrergic projections.

Entorhinal Cortex

Control animals displayed a low density of multipolar nitrergic neurons scattered across layers II, III, V, and VI (Fig. 3C1; Table 1). Layer III contained many dendritic profiles, and strong neuropilar staining was evident in layers III and V (Table 2).

In MDA rats, no significant changes in nitrergic neuron density were observed, indicating relative preservation in this cortical gateway. Likewise, neuropilar labeling remained moderate-to-strong across layers, confirming the stability of nitrergic afferents in this region.

Distribution of nNOS immunoreactivity in the habenular complexes and basolateral nuclear complex of the amygdala

Habenular Complexes

nNOS-IR neurons were more numerous in the MHb than in the LHb in controls (Fig. 4A1–C1; Table 1), although neuropilar staining was strongest in the lateral complex (Table 2). In MDA rats, overall MHb nitrergic neuron density was unchanged compared with CTL rats. In the LHb, when considering both hemispheres together, no overall differences were observed between CTL and MDA rats. However, a clear hemispheric effect emerged. In the LHb, a significant asymmetry was observed between hemispheres within the MDA group ($t_{(2)} = -7.36$, $p < 0.05$, $d = 4.25$). Significant differences were also detected between CTL and MDA rats in both the right ($t_{(2.86)} = -3.41$, $p < 0.05$, $d = 2.78$) and left hemispheres ($t_{(3.45)} = 6.32$, $p < 0.05$, $d = 5.16$). Overall, these findings indicate an opposite pattern of lateralized response of LHb nitrergic neurons to MDA paradigm (Table 1).

Neuropilar density remained moderate in the MHb and high in the LHb of MDA rats (Table 2), indicating that axonal terminals and dendritic arbors of nitrergic neurons are relatively resistant to MDA-induced injury.

Basolateral Nuclear Complex of the Amygdala

In controls, moderate densities of nitrergic neurons and dense fibers were observed throughout the lateral, basal, and accessory basal nuclei (Figs. 5-6) (Tables 1–2). The lateral nucleus had the highest density, while the basal and accessory basal nuclei contained fewer scattered neurons. Immunoreactive cells displayed ovoid, fusiform, multipolar, and bipolar morphologies, consistent with non-pyramidal interneurons.

Neuropilar staining was moderate in all nuclei, with no significant differences between MDA and control rats (Table 2). This pattern may indicate that the nitrergic network in the amygdala is less vulnerable to the effects of the induction of MDAs compared to hippocampal regions.

Discussion

The present study documents the presence of nitrergic neurons in the hippocampal–parahippocampal region and limbic structures, with a particularly high density of nitrergic neurons in the CA1 pyramidal cell layer and the MHb. In addition, we provided a preliminary overview of region- and hemisphere-specific nitrergic differences following repeated MDA epileptiform discharges induced by unilateral left PP electrical stimulation. While the DG, entorhinal cortex and basolateral amygdala appeared unaffected, we observed difference in CA1, CA3, subiculum and LHb. These findings may reflect acute region-specific effects of paroxysmal dentate activity, with selective vulnerability and NO signaling possibly influencing seizure susceptibility (Stringer and Lothman 1992).

Distribution of nitrergic neurons

Under control conditions, nitrergic neurons were abundant in the DG, especially in the polymorphic and granule cell layers, where they exhibited multipolar and fusiform morphologies consistent with interneurons (Jinno and Kosaka 2002, Liang, Zhang et al. 2013). In the hippocampus proper, neurons were concentrated in pyramidal and radiatum layers, fewer in oriens, and largely absent from lacunosum-moleculare, with occasional pyramidal cells showing weak staining as described previously (Vincent and Kimura 1992). The subiculum contained neurons across all layers with dense neuropilar staining, particularly in layer III, while the entorhinal cortex showed sparse multipolar cells in layers II-VI with prominent fiber plexuses in layers III and V as shown by (Vincent and Kimura 1992, Jinno and Kosaka 2002). Importantly, the predominance of interneuronal morphologies supports a role for NO in fine-tuning local inhibitory control, while selective pyramidal labeling indicates a possible contribution to long-range integration.

Within the amygdala, we corroborate previous evidence for moderate nitrergic density in the basolateral complex, especially in the lateral nucleus (Vincent and Kimura 1992, McDonald, Payne et al. 1993). The predominance of non-pyramidal morphologies suggests a role in inhibitory

regulation of excitability within amygdala networks, although the basolateral complex appeared largely resistant to acute MDA-induced changes.

A novel aspect of our work concerns the habenula, previously thought to lack nitrergic neurons in mammals, consistent with limited staining in rats (Vincent and Kimura 1992), in contrast to amphibians and reptiles, which show NADPH-d labeling in the MHb (Guglielmotti and Fiorino 1999). More recent rodent studies suggested a different scenario, with nNOS antibodies identifying nNOS-IR neurons in the LHb (Chen, Chen et al. 2023), and dense NOS-IR inputs from the entopeduncular nucleus (Miyamoto and Fukuda 2021). Here, we showed a gradient of nNOS-IR neurons across the Hb, with higher density in the MHb than LHb, indicating region-specific NO signaling relevant to habenular functions.

Effect of MDA on nitrergic neurons

To assess NOS changes across epileptic brain network areas, we used an acute kindling model reproducing key features of mTLE and employed the MDA paradigm (Stringer and Lothman 1992). MDA is a well-characterized model of reverberatory seizure activity within hippocampal-parahippocampal circuits and has been widely used to investigate the pharmacological modulation of hippocampal hyperexcitability, including NO signaling (Stringer and Erden 1990, Sardo, Carletti et al. 2006), 5-HT receptor ligands (Orban, Pierucci et al. 2013, Orban, Bombardi et al. 2014) and cannabinoids (Stringer and Lothman 1989, Stringer and Lothman 1992, Orban, Bombardi et al. 2014, Colangeli, Pierucci et al. 2017, Grillo, Fezza et al. 2021). Consistent with previous findings, MDA evoked by angular bundle stimulation under anesthesia produced bursts of dentate spikes with afterdischarges that progressively lengthened upon repetition (Stringer and Lothman 1992).

Comparison of sham control animals with MDA rats, and between the left (MDA-L) and stimulated (MDA-R) hemispheres, showed that the most pronounced reductions occurred ipsilateraly to stimulation, particularly in the stratum oriens of CA1/CA3. On the other hand, the CA3 pyramidal layer shows increase, which may reflect asymmetric (contralateral) remodeling. The subiculum exhibited a small reduction, driven primarily by a contralateral hemispheric decrease. In contrast, the entorhinal cortex, the basolateral amygdala and the Hb remained largely unaffected. Although not statistically significant, our findings in DG showing a trend toward a reduction of nitrergic neurons following MDA are consistent with those reported by Stringer and Erden (Stringer and Erden 1990), who described a selective loss of NADPH-d-IR neurons in the subgranular/hilar DG after repeated MDA seizures, by demonstrating hemisphere-specific vulnerability following unilateral stimulation. Overall, our data indicate that hippocampal nitrergic neurons are differentially sensitive to seizure-induced hyperactivation, with lateralized effects largely absent in adjacent cortical and subcortical regions. Importantly, even a short series of 24 epileptiform discharges delivered at 10-min intervals

is sufficient to disrupt nitrergic signaling in key hippocampal output nodes (subiculum) and inhibitory microcircuits (oriens interneurons), suggesting a mechanistic substrate for enhanced hyperexcitability.

The reduction of nitrergic neurons aligns with the reduced hippocampal nNOS expression reported in TLE patients and with the low levels of hilar nNOS described in animal models of SE (Zhu, Zhou et al. 2025). The selective vulnerability of nitrergic neurons in the DG hilus and CA1/CA3 oriens is particularly relevant to seizure generation. These interneuron populations are strategically positioned to regulate excitatory drive from the entorhinal cortex and Schaffer collaterals, respectively (Freund and Antal 1988, Freund and Buzsáki 1996). Their selective loss reduces inhibitory control and NO-mediated modulation, thereby promoting hyperexcitability (Zhu, Zhou et al. 2025). The paradoxical increase in nitrergic neurons in the CA3 pyramidal layer may reflect a compensatory response, perhaps through upregulation of nNOS in non-traditional cell types (Valtschanoff, Weinberg et al. 1993, Blackshaw, Eliasson et al. 2003), or could represent transient immunohistochemical changes rather than true neurogenesis. Further studies employing stereological quantification and co-labeling with interneuron markers are needed to clarify this observation (Buckmaster and Wen 2011, Franz, Barheier et al. 2023). Together with our data, published findings suggest that NO in MDA both weakens inhibitory restraint by reducing nitrergic interneurons and, through residual or compensatory signaling, interacts with cannabinoid pathways to fine-tune seizure susceptibility (Carletti, Gambino et al. 2017, Colangeli, Pierucci et al. 2017, Grillo, Fezza et al. 2021). This dualism may help reconcile conflicting reports on NO as either a pro-(Sardo, Carletti et al. 2006) or anti-convulsant factor in the MDA model (Stringer and Erden 1990), noting that the former evidence was obtained using a modified MDA protocol without kindling. Rather than exerting a uniform action, NO likely functions as a context-dependent modulator, with its effects determined by cellular source, receptor interactions, and the stage of epileptogenic progression. For instance nitrergic neurons are overexpressed in the hippocampus of mice with pilocarpine (PILO)-induced SE and nNOS knockout ameliorates cognitive impairment and neuroinflammation by enhancing CREB-mediated neuropeptide Y expression in TLE models (Yao, Hu et al. 2022). These discrepancies likely reflect differences in seizure models, brain regions engaged, and the degree of NOS inhibition achieved.

Although the hippocampus remains central to TLE pathology, epileptogenesis involves broader limbic networks. Among them, the amygdala is a major seizure hub, implicated in both epileptogenic and psychiatric comorbidities in TLE (Mourre, Makhalova et al. 2025). The amygdala has reciprocal excitatory connections with the hippocampus (Pitkänen, Pikkarainen et al. 2000), and amygdala kindling in rodents recruits hippocampal circuits, producing TLE (Goddard 1967) and it is activated 60 min after PILO in rat model of TLE (Sinel'nikova, Shubina et al. 2013). Connectivity of amygdalar

subnuclei with hippocampal and cortical regions rises during seizures (Aung, Tang et al. 2025), amygdalar asymmetry predicts seizure laterality (Venkatesan, Babajani-Feremi et al. 2025), and in late-onset TLE, enlargement of the amygdala-hippocampal transition zone correlates with interictal discharges and memory deficits (Takeyama, Matsumoto et al. 2025).

In our study, the basolateral amygdala nuclei exhibited similar nitrergic neuron densities across groups, suggesting relative preservation under acute MDA conditions. The lack of change in nitrergic neurons here does not preclude later amygdalar involvement in chronic epilepsy but emphasizes the hippocampus and subiculum as primary early targets.

As with the habenula, the MHb is activated during pentylenetetrazole-induced epileptogenesis (Bastlund, Berry et al. 2005), but its nitrergic neuron density remained unchanged in our acute model. The LHb also modulates limbic seizures through hippocampal-brainstem circuits involving the dorsal raphe and basal ganglia (Patel, Millan et al. 1988). Its early activation precedes hippocampal recruitment and peaks during PILO-induced status epilepticus (Sinel'nikova, Shubina et al. 2013). The LHb may thus influence limbic excitability and contribute to extrahippocampal seizure propagation through its nitrergic neurons (Chen, Chen et al. 2023). Here, we observed an increased nitrergic population in the right LHb, ipsilateral to electrical stimulated hemisphere compared to the left side. This increase was also higher than in controls, consistent with the evidence of elevated nNOS-IR neurons in the LHb in a mouse model of depression (Chen, Chen et al. 2023). This suggests that unilateral PP stimulation may alter NO-dependent modulation in the LHb, potentially contributing to asymmetrical seizure propagation and/or mood disturbances in mTLE. Further studies are needed to define the role of habenular nitrergic circuits in epilepsy. Our findings, together with pharmacological work in the MDA model (Stringer and Erden 1990, Sardo, Carletti et al. 2006) and PILO-induced status epilepticus (Zhu, Zhou et al. 2025), point to NO signaling as a key regulator of hyperexcitability. The acute loss of nitrergic interneurons in the CA fields may serve as the initiating event, while sustained NO deficiency drives long-term circuit remodeling. Targeting this pathway, through selective nNOS modulation, NO donor administration, or combined CB manipulation, could provide novel antiepileptogenic strategies.

This study was intended as a preliminary exploratory investigation and therefore has some limitations, including the non-stereological nature of the cell counts and the small sample size. Nevertheless, the relatively large effect sizes observed in several comparisons suggest that the findings may reflect biologically meaningful differences.

Conclusion

In summary, these results suggest that hippocampal nitrergic interneurons display a selective vulnerability to MDA seizures, with an acute reduction in the CA1/CA3 stratum oriens and an

increase in the CA3 pyramidal cell layer, potentially reflecting a disruption of NO-mediated inhibitory control and a shift toward hyperexcitability. Adjacent regions, including the basolateral amygdala and MHb, were largely unaffected. In contrast, the LHb exhibited a marked hemispheric asymmetry, with an increase in the stimulated right LHb and a decrease in the left LHb, a pattern that may contribute to seizure and/or mood-related comorbidities. These data are promising and warrant further studies into nitrergic pathways as potential therapeutic targets for TLE.

References

Alabadí, J. A., J. L. Thibault, E. Pinard, J. Seylaz and F. Lasbennes (1999). "7-Nitroindazole, a selective inhibitor of nNOS, increases hippocampal extracellular glutamate concentration in status epilepticus induced by kainic acid in rats." Brain Res **839**(2): 305-312.

Aung, T., L. W. Tang, J. Ho, L. C. Henry, N. Ikegaya, M. Modo and J. Gonzalez Martinez (2025). "Differential functional connectivity of amygdala in drug-resistant temporal lobe epilepsy." Epilepsia.

Bastlund, J. F., D. Berry and W. P. Watson (2005). "Pharmacological and histological characterisation of nicotine-kindled seizures in mice." Neuropharmacology **48**(7): 975-983.

Blackshaw, S., M. J. L. Eliasson, A. Sawa, C. C. Watkins, D. Krug, A. Gupta, T. Arai, R. J. Ferrante and S. H. Snyder (2003). "Species, strain and developmental variations in hippocampal neuronal and endothelial nitric oxide synthase clarify discrepancies in nitric oxide-dependent synaptic plasticity." Neuroscience **119**(4): 979-990.

Bredt, D. S., C. E. Glatt, P. M. Hwang, M. Fotuhi, T. M. Dawson and S. H. Snyder (1991). "Nitric oxide synthase protein and mRNA are discretely localized in neuronal populations of the mammalian CNS together with NADPH diaphorase." Neuron **7**(4): 615-624.

Buckmaster, P. S. and X. Wen (2011). "Rapamycin suppresses axon sprouting by somatostatin interneurons in a mouse model of temporal lobe epilepsy." Epilepsia **52**(11): 2057-2064.

Carletti, F., G. Gambino, V. Rizzo, G. Ferraro and P. Sardo (2017). "Neuronal nitric oxide synthase is involved in CB/TRPV1 signalling: focus on control of hippocampal hyperexcitability." Epilepsy research **138**: 18-25.

Carter, D. S., L. S. Deshpande, A. Rafiq, S. Sombati and R. J. DeLorenzo (2011). "Characterization of spontaneous recurrent epileptiform discharges in hippocampal-entorhinal cortical slices prepared from chronic epileptic animals." Seizure **20**(3): 218-224.

Chachlaki, K. and V. Prevot (2020). "Nitric oxide signalling in the brain and its control of bodily functions." Br J Pharmacol **177**(24): 5437-5458.

Chen, W., Y. Chen, M. S. Aslam, J. Shen, T. Tong, S. Yan, W. Cheng, Z. Huang, J. Li, S. Liu, J. Li, J. Zeng, M. Li, Z. You and X. Meng (2023). "The effect of acupuncture on lateral habenular nucleus and intestinal microflora in depression model rats." Behavioural Brain Research **455**: 114627.

Colangeli, R., M. Pierucci, A. Benigno, G. Campiani, S. Butini and G. Di Giovanni (2017). "The FAAH inhibitor URB597 suppresses hippocampal maximal dentate afterdischarges and restores seizure-induced impairment of short and long-term synaptic plasticity." Scientific reports **7**(1): 11152.

De Sarro, G., B. S. Meldrum, A. De Sarro and S. Patel (1992). "Excitatory neurotransmitters in the lateral habenula and pedunculopontine nucleus of rat modulate limbic seizures induced by pilocarpine." Brain Research **591**(2): 209-222.

Del-Bel, E. A., P. R. Oliveira, J. A. Oliveira, P. K. Mishra, P. C. Jobe and N. Garcia-Cairasco (1997). "Anticonvulsant and proconvulsant roles of nitric oxide in experimental epilepsy models." Braz J Med Biol Res **30**(8): 971-979.

Di Giovanni, G., I. García, R. Colangeli, M. Pierucci, M. L. Rivadulla, E. Soriano, M. Chioua, L. Della Corte, M. Yáñez and P. De Deurwaerdère (2014). "N-(furan-2-ylmethyl)-N-methylprop-2-yn-1-amine (F2 MPA): A

Potential Cognitive Enhancer with MAO Inhibitor Properties." CNS neuroscience & therapeutics **20**(7): 633-640.
Feigin, V. L., T. Vos, B. S. Nair, S. I. Hay, Y. H. Abate, A. H. Abd Al Magied, S. Abd ElHafeez, A. Abdelkader, M.-A. Abdollahifar and A. Abdullahi (2025). "Global, regional, and national burden of epilepsy, 1990–2021: a systematic analysis for the Global Burden of Disease Study 2021." The Lancet Public Health **10**(3): e203-e227.
Franz, J., N. Barheier, H. Wilms, S. Tulke, C. A. Haas and U. Häussler (2023). "Differential vulnerability of neuronal subpopulations of the subiculum in a mouse model for mesial temporal lobe epilepsy." Front Cell Neurosci **17**: 1142507.
Freund, T. F. and M. Antal (1988). "GABA-containing neurons in the septum control inhibitory interneurons in the hippocampus." Nature **336**(6195): 170-173.
Freund, T. F. and G. Buzsáki (1996). "Interneurons of the hippocampus." hippocampus **6**(4): 347-470.
Goddard, G. V. (1967). "Development of epileptic seizures through brain stimulation at low intensity." Nature **214**(5092): 1020-1021.
Grillo, A., F. Fezza, G. Chemi, R. Colangeli, S. Brogi, D. Fazio, S. Federico, A. Papa, N. Relitti and R. Di Maio (2021). "Selective fatty acid amide hydrolase inhibitors as potential novel antiepileptic agents." ACS Chemical Neuroscience **12**(9): 1716-1736.
Guglielmotti, V. and L. Fiorino (1999). "Nitric oxide synthase activity reveals an asymmetrical organization of the frog habenulae during development: a histochemical and cytoarchitectonic study from tadpoles to the mature Rana esculenta, with notes on the pineal complex." Journal of Comparative Neurology **411**(3): 441-454.
Hollis, A. and J. R. Lukens (2025). "Role of inflammasomes and neuroinflammation in epilepsy." Immunological Reviews **329**(1): e13421.
Jinno, S. and T. Kosaka (2002). "Patterns of expression of calcium binding proteins and neuronal nitric oxide synthase in different populations of hippocampal GABAergic neurons in mice." Journal of Comparative Neurology **449**(1): 1-25.
Liang, Z., L. Zhang, X. Wang, F. Gao, X. Wang, S. Zhou, S. Yu and R.-Z. Zhan (2013). "Distribution and neurochemical features of neuronal nitric oxide synthase-expressing interneurons in the rat dentate gyrus." Brain research **1505**: 11-21.
McDonald, A. J., D. R. Payne and F. Mascagni (1993). "Identification of putative nitric oxide producing neurons in the rat amygdala using NADPH-diaphorase histochemistry." Neuroscience **52**(1): 97-106.
Miyamoto, Y. and T. Fukuda (2021). "The habenula-targeting neurons in the mouse entopeduncular nucleus contain not only somatostatin-positive neurons but also nitric oxide synthase-positive neurons." Brain Struct Funct **226**(5): 1497-1510.
Mourre, H., J. Makhalova, L. Soncin, E. Garnier, H. Dary, A. Le Troter, R. A. M. Haast, B. Testud, M. Arthuis, S. M. Villalon, S. Lagarde, F. Pizzo, C. Bénar, J. P. Ranjeva, M. Guye and F. Bartolomei (2025). "Nuclei-Specific Amygdala Enlargement Is Linked to Psychiatric Comorbidities in Drug-Resistant Focal Epilepsy." Ann Clin Transl Neurol **12**(7): 1395-1407.
Orban, G., C. Bombardi, A. Marino Gammazza, R. Colangeli, M. Pierucci, C. Pomara, M. Pessia, F. Bucchieri, B. Arcangelo and I. Smolders (2014). "Role (s) of the 5-HT 2C Receptor in the Development of Maximal Dentate Activation in the Hippocampus of Anesthetized Rats." CNS neuroscience & therapeutics **20**(7): 651-661.
Orban, G., M. Pierucci, A. Benigno, M. Pessia, S. Galati, M. Valentino, R. Muscat and G. Di Giovanni (2013). "High dose of 8-OH-DPAT decreases maximal dentate gyrus activation and facilitates granular cell plasticity in vivo." Experimental brain research **230**(4): 441-451.
Park, K. I. (2024). "Understanding epileptogenesis from molecules to network alteration." Encephalitis **4**(3): 47-54.
Patel, S., M. H. Millan and B. S. Meldrum (1988). "Decrease in excitatory transmission within the lateral habenula and the mediodorsal thalamus protects against limbic seizures in rats." Experimental neurology **101**(1): 63-74.
Paxinos, G. and C. Watson (2004). The rat brain in stereotaxic coordinates-The New Coronal Set, Elsevier.
Pierucci, M., S. Galati, M. Valentino, V. Di Matteo, A. Benigno, A. Pitruzzella, R. Muscat and G. Di Giovanni (2011). "Nitric oxide modulation of the basal ganglia circuitry: therapeutic implication for Parkinson's disease and other motor disorders." CNS Neurol Disord Drug Targets **10**(7): 777-791.

Pitkänen, A., M. Pikkarainen, N. Nurminen and A. Ylinen (2000). "Reciprocal connections between the amygdala and the hippocampal formation, perirhinal cortex, and postrhinal cortex in rat. A review." Ann N Y Acad Sci **911**: 369-391.
Ravizza, T., M. Scheper, R. Di Sapia, J. Gorter, E. Aronica and A. Vezzani (2024). "mTOR and neuroinflammation in epilepsy: implications for disease progression and treatment." Nat Rev Neurosci **25**(5): 334-350.
Sardo, P., F. Carletti, S. D'Agostino, V. Rizzo and G. Ferraro (2006). "Involvement of nitric oxide-soluble guanylyl cyclase pathway in the control of maximal dentate gyrus activation in the rat." J Neural Transm (Vienna) **113**(12): 1855-1861.
Sinel'nikova, V. V., L. V. Shubina, M. V. Gol'tyaev, E. V. Loseva and V. F. Kichigina (2013). "Detection of c-Fos Expression in the Brains of Animals with a Pilocarpine Model of Temporal Lobe Epilepsy." Neuroscience and Behavioral Physiology **43**(9): 1084-1091.
Stringer, J. L. and F. Erden (1990). "In the hippocampus in vivo, nitric oxide does not appear to function as an endogenous antiepileptic agent." Experimental brain research **105**(3): 391-401.
Stringer, J. L. and E. W. Lothman (1989). "Maximal dentate gyrus activation: characteristics and alterations after repeated seizures." Journal of neurophysiology **62**(1): 136-143.
Stringer, J. L. and E. W. Lothman (1990). "Maximal dentate activation: a tool to screen compounds for activity against limbic seizures." Epilepsy research **5**(3): 169-176.
Stringer, J. L. and E. W. Lothman (1992). "Reverberatory seizure discharges in hippocampal-parahippocampal circuits." Experimental neurology **116**(2): 198-203.
Takechi, K., K. Suemaru, T. Kiyoi, A. Tanaka and H. Araki (2016). "The α4β2 nicotinic acetylcholine receptor modulates autism-like behavioral and motor abnormalities in pentylenetetrazol-kindled mice." European Journal of Pharmacology **775**: 57-66.
Takeyama, H., R. Matsumoto, K. Usami, M. Tojima, A. Shima, M. Honda, M. Sakamoto, T. Murai, K. Hayashi and Y. Fushimi (2025). "Late-onset temporal lobe epilepsy: Enlarged amygdala-hippocampus indicates interictal epileptic activity at electroencephalography and memory impairment." Epileptic Disorders.
Téllez-Zenteno, J. F. and L. Hernández-Ronquillo (2012). "A review of the epidemiology of temporal lobe epilepsy." Epilepsy research and treatment **2012**(1): 630853.
Valtschanoff, J. G., R. J. Weinberg, V. N. Kharazia, M. Nakane and H. H. H. W. Schmidt (1993). "Neurons in rat hippocampus that synthesize nitric oxide." Journal of Comparative Neurology **331**(1): 111-121.
Venkatesan, S., A. Babajani-Feremi, K. Patel, S. N. Roper and G. Kalamangalam (2025). "Amygdalar volume asymmetry informs laterality in temporal lobe epilepsy: MRI-SEEG study." Seizure: European Journal of Epilepsy **126**: 58-63.
Vincent, S. R. and H. Kimura (1992). "Histochemical mapping of nitric oxide synthase in the rat brain." Neuroscience **46**(4): 755-784.
Wang, X., Y. Zhang, W. Cheng, Y. Gao and S. Li (2021). "Decreased excitatory drive onto hilar neuronal nitric oxide synthase expressing interneurons in chronic models of epilepsy." Brain Research **1764**: 147467.
Yao, Y., Y. Hu, J. Yang, C. Zhang, Y. He, H. Qi, Y. Zeng, A. Zhang, X. Liu and X. Zhu (2022). "Inhibition of neuronal nitric oxide synthase protects against hippocampal neuronal injuries by increasing neuropeptide Y expression in temporal lobe epilepsy mice." Free Radical Biology and Medicine **188**: 45-61.
Zhu, X. H., Y. P. Zhou, Q. Zhang, M. Y. Zhu, X. W. Song, J. Li, J. Chen, Y. Shi, K. J. Sun, Y. J. Zhang, J. Zhang, T. Xia, B. S. Huang, F. Meng and Q. G. Zhou (2025). "A novel anti-epileptogenesis strategy of temporal lobe epilepsy based on nitric oxide donor." EMBO Mol Med **17**(1): 85-111.

FIGURES LEGEND

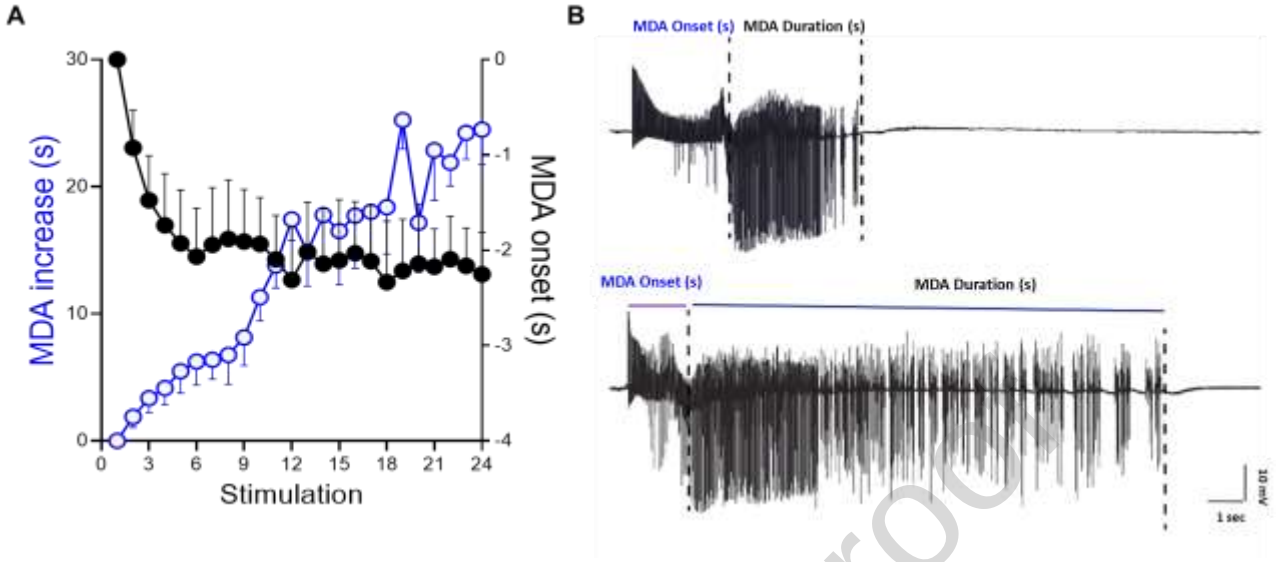

Figure 1

Representative electrophysiological recordings of onset and duration of maximal dentate activation (MDA) in alternating current (AC) mode from the dentate gyrus of the hippocampus of a urethane-anesthetized rat.

(A) The increase and time to onset of MDA were measured for each stimulus train. MDA was defined as the prolonged, high-frequency, high-amplitude population spike (PS) activity that follows perforant-path stimulation and reflects pathological activation of the dentate gyrus. Values were normalized, averaged, and plotted (± SEM) against the stimulus number. Each circle represents the mean value obtained from six animals.

(B) The time to MDA onset is defined as the interval between the beginning of the stimulus train and the midpoint of the maximal amplitude of the population spikes (PSs). MDA was induced by a 10 s, 20 Hz electrical stimulation with intensities ranging from 200 to 1000 μA. MDA duration corresponds to the total length of the sustained epileptiform PS burst following the stimulus train. Note the marked increase in MDA duration between the first and the 24th stimulus.

Figure 2. Distribution of nNOS immunoreactivity in the hippocampal formation of Control (A1, B1, C1) and MDA (A2, B2, C2) rats. (A1–A2) dentate gyrus and hippocampus proper, (B1–B2) dentate gyrus, and (C1–C2) CA1 field. The overall staining pattern in Control rats is similar to that observed in MDA rats. Scale bars: 400 μm in A1 (applies to A1, A2); 100 μm in B1 (applies to B1–C2). Abbreviations: GL, granule cell layer; ML, molecular layer; PCL, polymorphic cell layer; PL, pyramidal cell layer; SLM, stratum lacunosum-moleculare; SO, stratum oriens; SR, stratum radiatum.

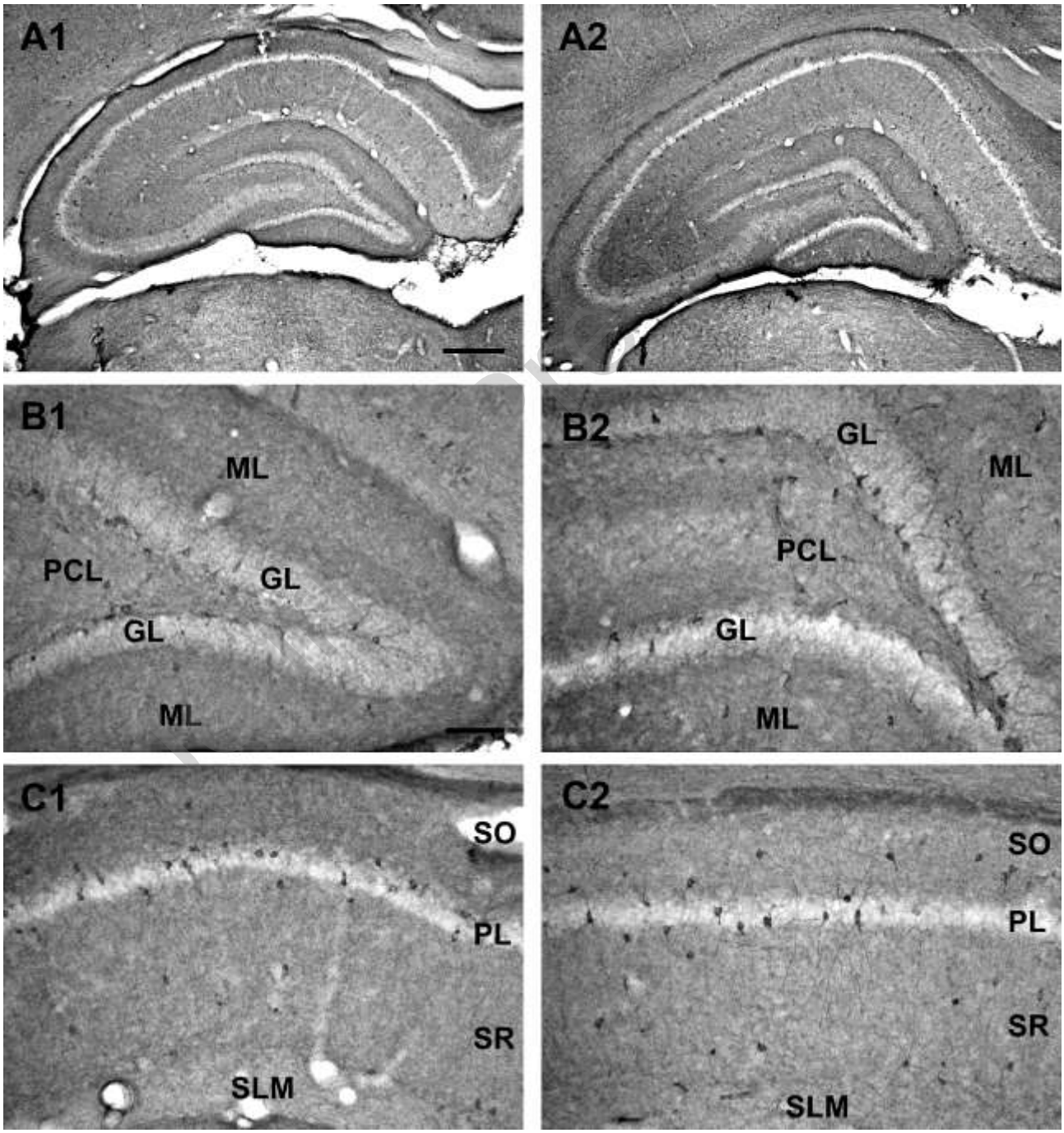

Figure 3. Distribution of nNOS immunoreactivity in the hippocampus proper and entorhinal cortex of Control (A1, B1, C1) and MDA (A2, B2, C2) rats. (A1–A2) CA3 field, (B1–B2) subiculum, and (C1–C2) entorhinal cortex. The overall staining pattern in Control rats is similar to that observed in MDA rats. Scale bars: 100 µm in A1 (applies to A1–B2); 50 µm in C1 (applies to C1, C2). Abbreviations: PCL, pyramidal cell layer; SO, stratum oriens; SR, stratum radiatum.

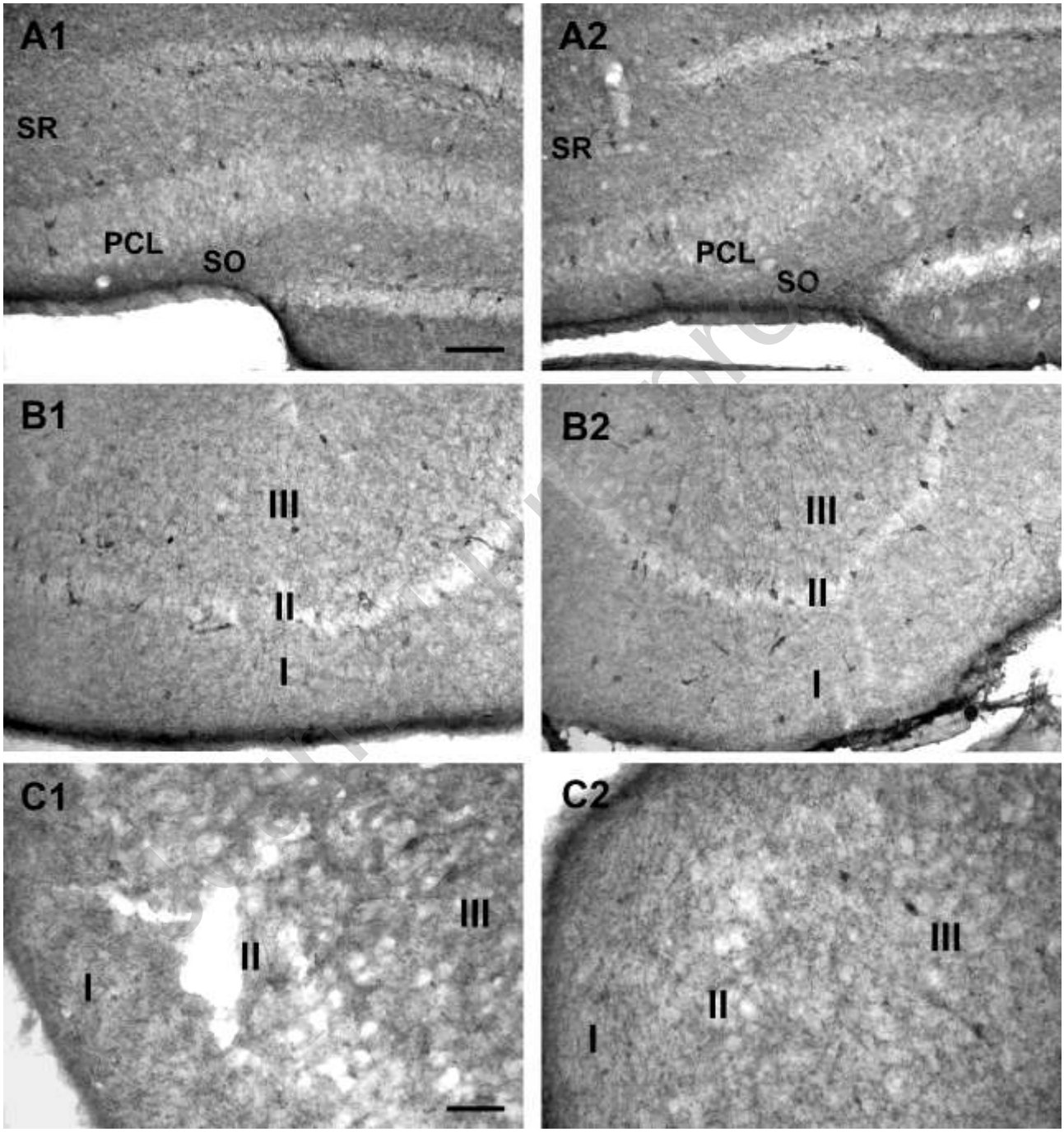

Figure 4. Distribution of nNOS immunoreactivity in the habenular complexes of Control (A1, B1, C1) and MDA (A2, B2, C2) rats. In both the medial and lateral habenula, the overall staining pattern in Control rats is similar to that observed in MDA rats. Scale bars: 400 µm in A1 (applies to A1, A2); 100 µm in B1 (applies to B1, B2); 50 µm in C1 (applies to C1, C2). Abbreviations: LHb, lateral habenular complex; MHb, medial habenular complex.

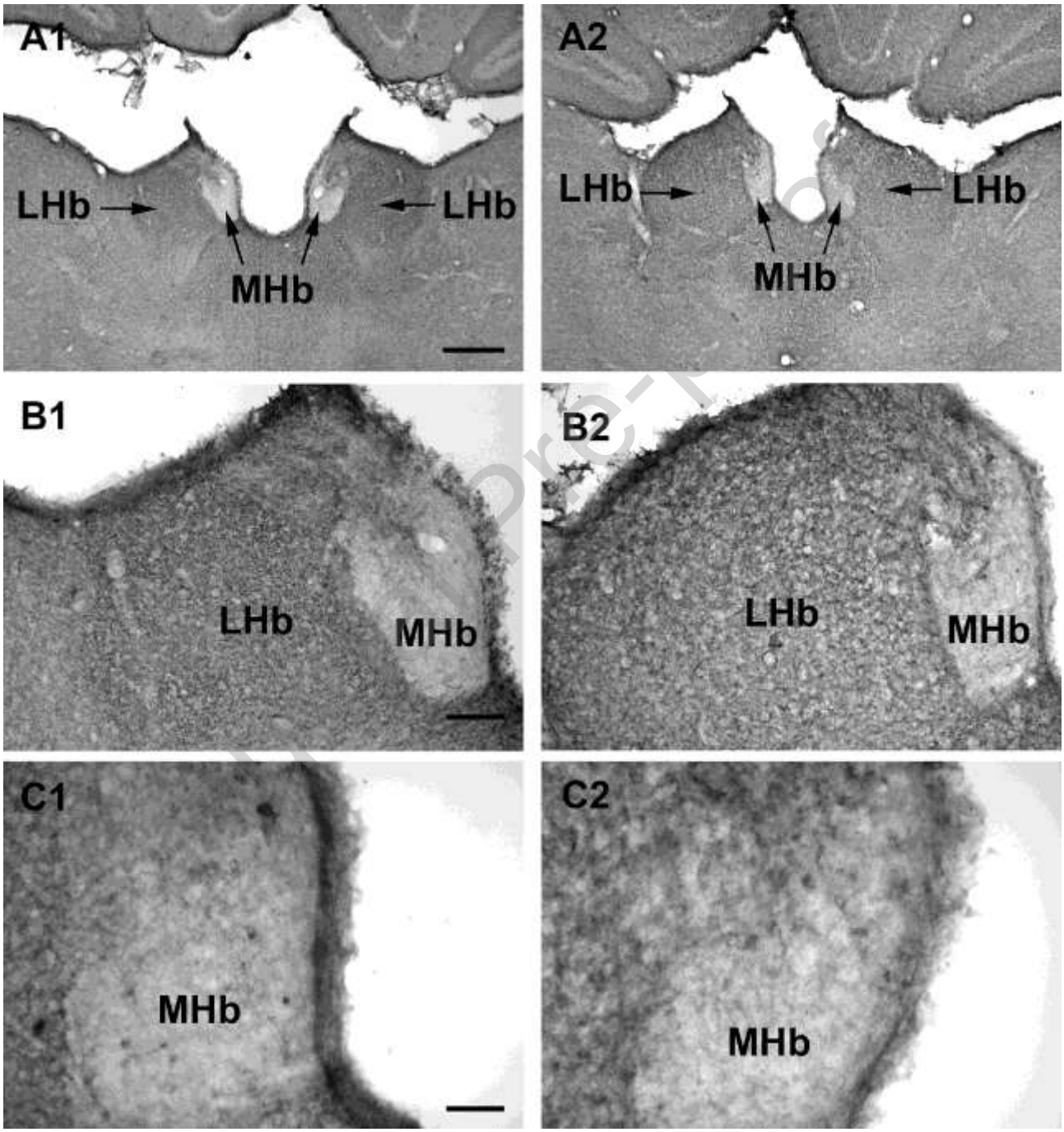

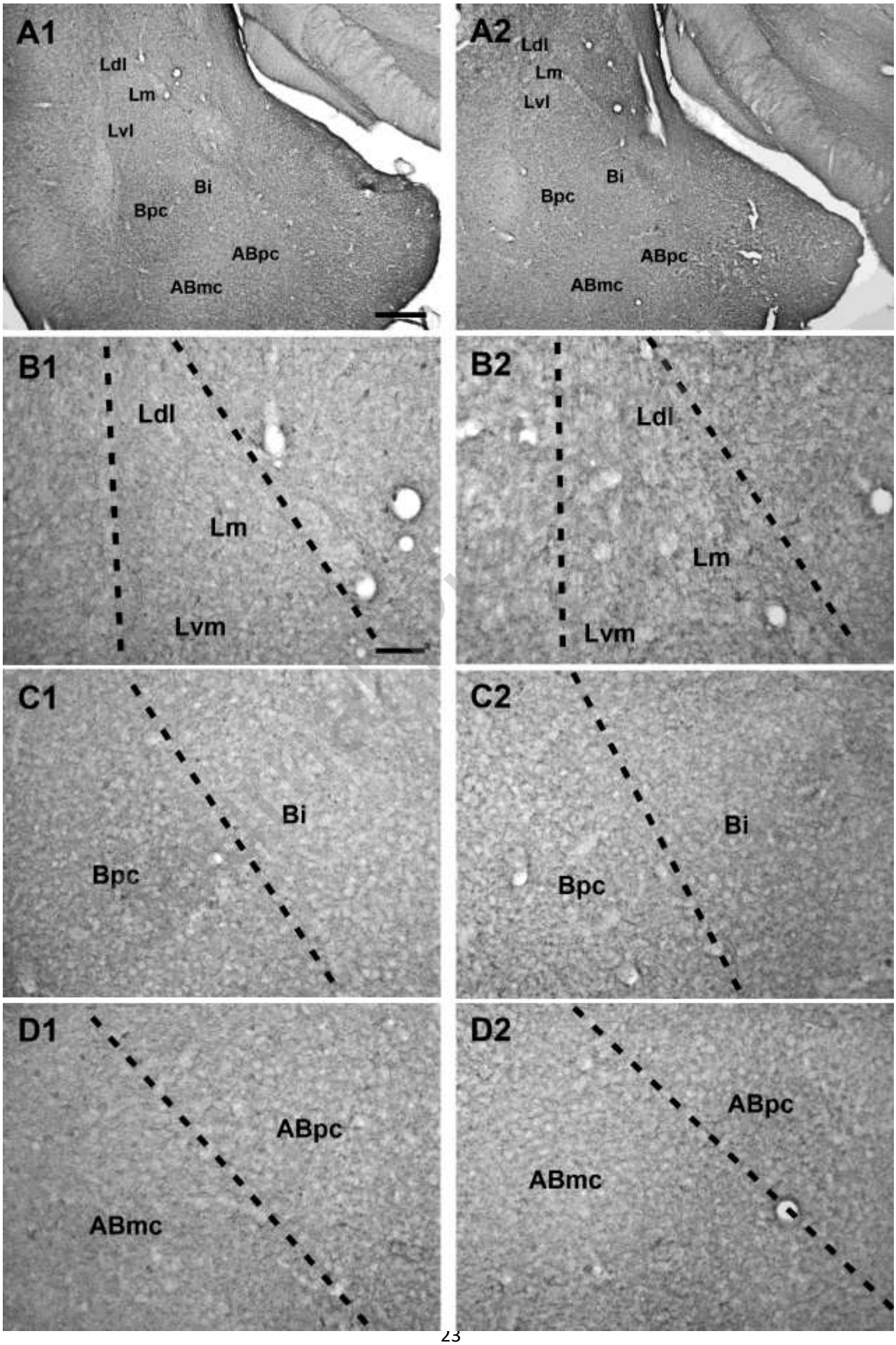
A1
Ldl
Lm
Lvl
Bi
Bpc
ABpc
ABmc
A2
Ldl
Lm
Lvl
Bi
Bpc
ABpc
ABmc
B1
Ldl
Lm
Lvm
B2
Ldl
Lm
Lvm
C1
Bi
Bpc
C2
Bi
Bpc
D1
ABpc
ABmc
D2
ABpc
ABmc

Figure 5. Distribution of nNOS immunoreactivity in the basolateral nuclear complex of the amygdala of Control (A1, B1, C1, D1) and MDA (A2, B2, C2, D2) rats. (A1–A2) basolateral nuclear complex, (B1–B2) lateral nucleus, (C1–C2) basal nucleus, and (D1–D2) accessory basal nucleus. The overall staining pattern in Control rats is similar to that observed in MDA rats. Scale bars: 400 µm in A1 (applies to A1, A2); 100 µm in B1 (applies to B1–D2). Abbreviations: Ldl, dorsolateral division of the lateral nucleus; Lm, medial division of the lateral nucleus; Lvl, ventrolateral division of the lateral nucleus; Bpc, parvicellular division of the basal nucleus; Bi, intermediate division of the basal nucleus; ABmc, magnocellular division of the accessory basal nucleus; ABpc, parvoellular division of the accessory basal nucleus.

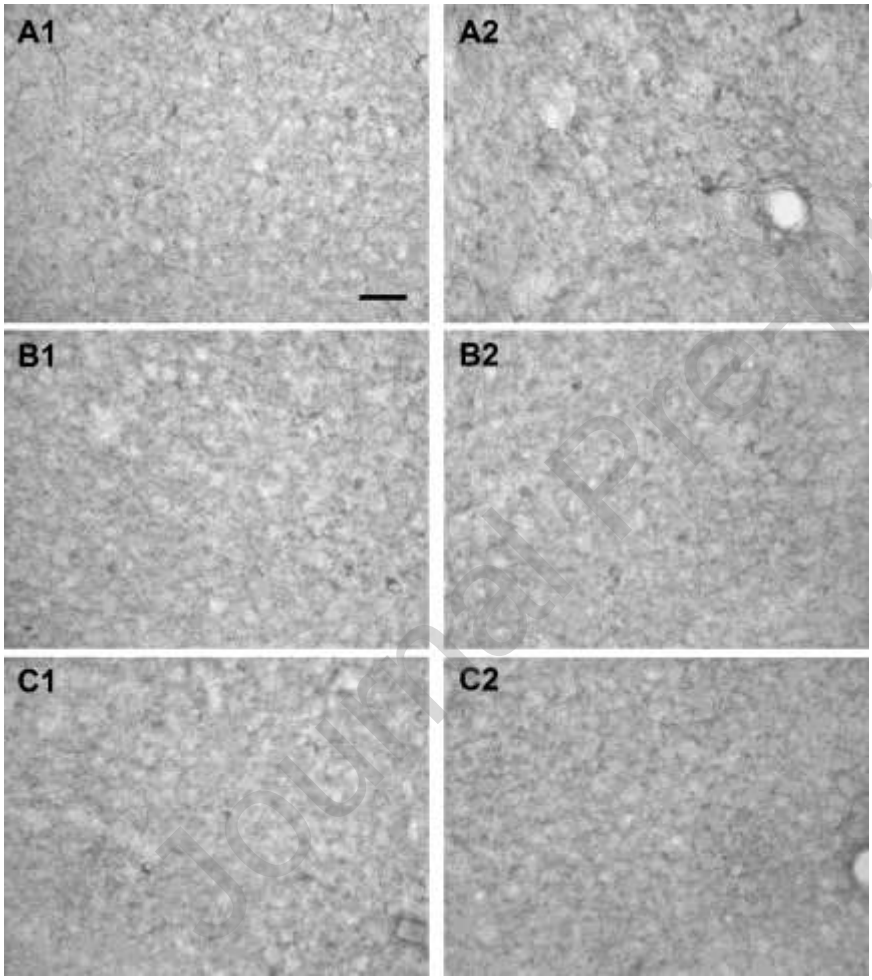

Figure 6. Distribution of nNOS immunoreactivity in the basolateral nuclear complex of the amygdala of Control (A1, B1, C1) and MDA (A2, B2, C2) rats. (A1–A2) medial subdivision of the lateral nucleus, (B1–B2) intermediate division of the basal nucleus, and (C1–C2) magnocellular division of the accessory basal nucleus. The overall staining pattern in Control rats is similar to that observed in MDA rats. Scale bar: 50 µm in A1 (applies to A1–C2).

Table 1. The density of nitrergic neurons in control and MDA rats

Area	Layer	CTL	MDA	MDA-L	MDA-R
DENTATE GYRUS					
	Polymorphic cell layer	104.3 ± 47.4	69.7 ± 12.2	67.7 ± 10.4	70.7 ± 20.3
	Granule cell layer	165.3 ± 79.8	134 ± 29.6	170.3 ± 37	97.3 ± 22.5
	Molecular layer	24 ± 15.5	18 ± 14.4	13.3 ± 6.4	22.3 ± 22.1
HIPPOCAMPUS PROPER					
CA1	**Stratum oriens**	71.3 ± 26.4	45.3 ± 12.7*	58.7 ± 12.7	31.3 ± 18.6#
	Pyramidal cell layer	313.7 ± 80.7	334.3 ± 132.5	327 ± 245	341.3 ± 42.7
	Stratum radiatum	49.3 ± 3.5	61.3 ± 26.3	69 ± 22.6	53 ± 32.9
	Stratum lacunosum-moleculare	occasionally found	occasionally found	occasionally found	occasionally found
CA3	**Stratum oriens**	36 ± 31.3	9 ± 5.6*	9.7 ± 6.7#	8.3 ± 4.4#
	Pyramidal cell layer	61.7 ± 35.2	99.3 ± 28.5*	124.3 ±78.7#	74 ± 37
	Stratum radiatum	69 ± 46.9	93.7 ± 59.7	73 ± 35.3	113.7 ± 84.8
	Stratum lacunosum-moleculare	occasionally found	occasionally found	occasionally found	occasionally found
SUBICULUM					
		53 ± 7.1	44 ± 5.7*	37 ± 4.2#	50.5 ± 14.8

ENTORHINAL CORTEX					
		19 ± 5.7	18.3 ± 2.8	17.5 ± 3.5	20 ± 2.2
HABENULAR COMPLEXES					
	Medial habenula	203 ± 54.6	179 ± 66.6	200.7 ± 74.9	157 ± 65.1
	Lateral habenula	3.3 ± 2.9	3.3 ± 2.7	2 ± 1.5$^{\#}$	4.7 ± 2.1$^{\#\circ}$
BASOLATERAL NUCLEAR COMPLEX OF THE AMYGDALA					
	Lateral nucleus	66.2 ± 6.7	68.2 ± 7.1	67.3 ± 6.8	69.8 ± 7.2
	Basal nucleus	48.2 ± 4.9	46.3 ± 5.7	48.1 ± 5.2	44.3 ± 5.9
	Accessory basal nucleus	47.1 ± 5.6	44.2 ± 4.4	42.4 ± 4.3	46.7 ± 4.6

The density of nitrergic neurons is expressed as mean ± SD (cells/mm²). Statistical significance is indicated as follows: *$p < 0.05$ versus CTL; °$p < 0.05$ versus MDA-L; and $^{\#}p < 0.05$ versus the respective CTL-L or CTL-R. CTL refers to the control group (mean of left and right hemispheres), MDA to the maximal dentate activation group (mean of left and right hemispheres), MDA-L to the maximal dentate activation group in the left hemisphere (contralateral to stimulation), and MDA-R to the maximal dentate activation group in the right hemisphere (ipsilateral to stimulation).

Table 2. Density of nitrergic neuropil in control and MDA rats

Area	Layer	CTL	MDA	MDA-L	MDA-R
DENTATE GYRUS					
	Polymorphic cell layer	+ +	+ +	+ +	+ +
	Granule cell layer	+	+	+	+
	Molecular layer	+ +/+ + +	+ +/+ + +	+ +/+ + +	+ +/+ + +
HIPPOCAMPUS PROPER					
CA1	**Stratum oriens**	+ +/+ + +	+ +/+ + +	+ +/+ + +	+ +/+ + +
	Pyramidal cell layer	+	+	+	+
	Stratum radiatum	+ +	+ +	+ +	+ +
	Stratum lacunosum-moleculare	+/+ +	+/+ +	+/+ +	+/+ +
CA3	**Stratum oriens**	+ +/+ + +	+ +/+ + +	+ +/+ + +	+ +/+ + +
	Pyramidal cell layer	+	+	+	+
	Stratum radiatum	+ +	+ +	+ +	+ +
	Stratum lacunosum-moleculare	+/+ +	+/+ +	+/+ +	+/+ +
SUBICULUM					
		+/+ +/+ + +	+/+ +/+ + +	+/+ +/+ + +	+/+ +/+ + +
ENTORHINAL CORTEX					
		+ +/+ + +	+ +/+ + +	+ +/+ + +	+ +/+ + +
HABENULAR COMPLEXES					
	Medial habenula	+ +	+ +	+ +	+ +

	Lateral habenula	+ + +	+ + +	+ + +	+ + +
BASOLATERAL NUCLEAR COMPLEX OF THE AMYGDALA					
	Lateral nucleus	+/+ +	+/+ +	+/+ +	+/+ +
	Basal nucleus	+/+ +	+/+ +	+/+ +	+/+ +
	Accessory basal nucleus	+/+ +	+/+ +	+/+ +	+/+ +

The intensity of neuropil staining is expressed as +++ high, ++ moderate, + low. CTL refers to the control group (mean of left and right hemispheres), MDA to the maximal dentate activation group (mean of left and right hemispheres), MDA-L to the maximal dentate activation group in the left hemisphere (contralateral to stimulation), and MDA-R to the maximal dentate activation group in the right hemisphere (ipsilateral to stimulation). The intensity of neuropil staining is expressed as +++ high, ++ moderate, + low.

CRediT authorship contribution statement

Cristiano Bombardi: Investigation, Methodology, Visualization, Writing – review & editing. **Roberto Colangeli**: Investigation, Methodology, Visualization, Formal analysis, Software, Data curation. **Maurizio Casarrubea**: Writing –review & editing. **Philippe De Deurwaerdère**: Writing – review & editing. **Vincenzo Crunelli**: Writing – review & editing. **Giuseppe Di Giovanni**: Conceptualization, Supervision, Writing – review & editing.

Declaration of Competing Interest

The authors declare no conflict of interest.

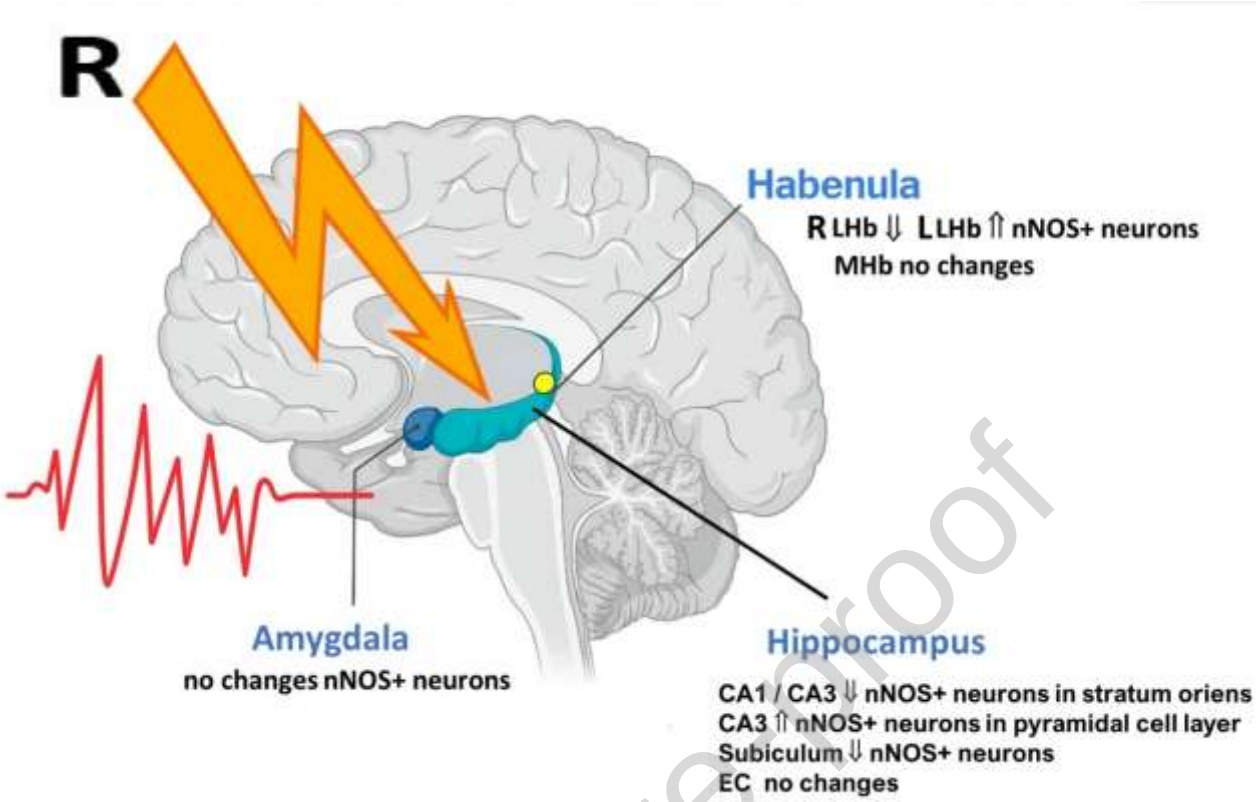

Graphical abstract